Electronic Supplementary Information

for

Rational Design of a Ruthenium–Cupin Complex

as an Artificial Ketone Reductase

Koki Matsumoto, Souto Kitazawa, Ryusei Matsumoto, Yoshitsugu Morita, and Nobutaka Fujieda*

Department of Applied Biological Chemistry, Graduate School of Agriculture, Osaka Metropolitan University, 1-1 Gakuen-cho, Naka-ku, Sakai-shi, Osaka 599-8531, Japan

Experimental Procedure

General Procedures. All reagents and solvents were purchased from commercial suppliers and used without further purification. ESI mass spectra were recorded on an Agilent LC/MSD system (G6125B). Chiral HPLC analysis was performed on an Agilent 1260 Infinity II system equipped with a UV diode-array detector and a polarimetric detector (OR-2090, JASCO Corp.) using chiral stationary-phase columns from DAICEL Co., Ltd. Retention times are reported in minutes.

Plasmids, Site-directed Mutagenesis, and Expression and Purification of Proteins. TM1459 constructs containing an N-terminal Strep-tag were expressed using pET30-based plasmids as previously described.[1] To prepare the plasmids for 1-His containing mutants, site-directed mutagenesis was performed on the TM1459 expression vector using inverse PCR with pairs of ~30-mer oligonucleotides (Macrogen Japan Co., Table S1, entries 1–14, SI), followed by DpnI digestion and self-ligation. For other mutants, overlap extension was employed instead of inverse PCR with pairs of ~40-mer oligonucleotides (Table S1, entries 15–32, SI). The absence of unwanted mutations was verified by Sanger sequencing (3730xl DNA Analyzer, Applied Biosystems). All mutants of TM1459 were purified according to established procedures.[1–3] Fractions containing TM1459 were pooled and concentrated by ultrafiltration (Vivaspin Turbo 15, Sartorius AG). Protein samples were stored at –80 °C until use. Purity was confirmed by SDS–PAGE (Fig. S1, SI). Protein concentration was determined from absorbance at 280 nm for homodimer.[4]

Crystallization. Purified apo-TM1459 was buffer-exchanged into 10 mM HEPES (pH 7.0) using a PD-10 column (Cytiva). An acetonitrile solution of $[Ru(p\text{-cymene})Cl_2]_2$ (150 μM, 1.5 equiv) was added to apo-TM1459 (100 μM) under N_2, followed by incubation for 16 h at room temperature. Excess metal ion was removed using a PD-10 column equilibrated with the same buffer. The protein was concentrated to 15 mg/mL and stored at –80 °C. Ru–TM1459 crystals were obtained by hanging-drop vapor diffusion.[1–3] Crystallization drops were prepared by mixing protein solution (2 μL) with 0.1 M MES (pH 6.0) containing 28 % (w/v) Jeffamine ED-2001 (1 μL). Crystals appeared within 1 week at 20 °C. Crystals were cryoprotected by soaking overnight in mother liquor containing 35 % (w/v) Jeffamine ED-2001.

Data Collection of X-Ray Diffraction and Structure Determination. Diffraction data were collected at BL44XU (SPring-8, Harima, Japan) using an EIGER X 16M detector (Dectris) at 100 K and a wavelength of 0.899995 Å. Data were processed using XDS. Data collection and refinement statistics are summarized in Table

S4. Structures were solved by molecular replacement using Phaser[5] with apo-TM1459 (PDB: 5WSD) as the search model. Models were refined iteratively with phenix.refine[6] and manually rebuilt in Coot. Final refinement was performed using SHELXL (2018/3)[7] manually rebuilding with Coot.[8] Anisotropic displacement parameters (ADP) were applied to all non-hydrogen atoms using RIGU[9] and SIMU instructions. In the case of R39M/58H/C106E, ADP was not applied to water molecules because the data-to-parameter ratio were not high enough. Geometric restraints for MES and Ru(*p*-cymene) ligands were generated with Grade Web Server (Global Phasing Ltd). Five percent of reflections were omitted for R_{free} calculation. Residues were well defined in the final electron density except for flexible loops (Table S5, SI). Metal–ligand distances and angles, including estimated errors, are summarized in Table S6. Ramachandran analysis (MolProbity)[10] showed no outliers. Final coordinates and structure factors have been deposited in the PDB (codes in Table S4). Secondary structures were assigned using DSSP.[11] Structural figures were generated with PyMOL (v3.1.0, Schrödinger LLC).

Asymmetric Hydrogenation of Ketone. A reaction vial (2 mL) was charged under N_2 with pH-adjusted sodium formate (100 μmol, 50 μL), [Ru(*p*-cymene)Cl_2]$_2$ (0.075 μmol, 10 μL), apo-TM1459 in 20 mM phosphate buffer (pH 6.5, 0.075 μmol), and acetonitrile containing 2,2,2-trifluoroacetophenone (8.5 μmol, 10 μL). The total volume was adjusted to 0.5 mL with Milli-Q water. The reaction mixture was stirred (600 rpm) at 40 °C in a sealed vial for 48 h under N_2. After the reaction, 1-naphthol was added as an internal standard. Products were extracted using hexane/isopropanol (97:3) and analyzed by chiral HPLC [CHIRALPAK IC-3, 5 μm, 4.6 × 250 mm, DAICEL Corp.] using authentic standards. Yields were determined from calibration curves of mole ratio versus area ratio.

Quantification of Formate Consumption and Analysis of Coupling Efficiency. Reaction mixtures were filtered through a centrifugal filter (Vivaspin 500, MWCO 10,000, Sartorius AS) and analyzed by an HPLC system (Prominence LC-20AD/SIL-20AC/SPD-20A; Shimadzu Corp.) equipped with an Asahipak ES-502N 7C column (9 μm, 7.5 × 100 mm, Resonac Corp.). A 10 mM citrate buffer (pH 3.9) containing 25 mM NaCl was used as an eluent to quantify unreacted formate anion.

Supporting References

1 N. Fujieda, H. Ichihashi, M. Yuasa, Y. Nishikawa, G. Kurisu and S. Itoh, *Angew Chem Int Ed*, 2020, 59, 7717–7720.

2 N. Fujieda, T. Nakano, Y. Taniguchi, H. Ichihashi, H. Sugimoto, Y. Morimoto, Y. Nishikawa, G. Kurisu and S. Itoh, *J Am Chem Soc*, 2017, 139, 5149–5155.

3 R. Matsumoto, S. Yoshioka, M. Yuasa, Y. Morita, G. Kurisu and N. Fujieda, *Chem Sci*, 2023, 14, 3932–3937.

4 S. C. Gill and P. H. von Hippel, *Anal Biochem*, 1989, 182, 319–326.

5 A. J. McCoy, R. W. Grosse-Kunstleve, P. D. Adams, M. D. Winn, L. C. Storoni and R. J. Read, *J Appl Crystallogr*, 2007, 40, 658–674.

6 P. D. Adams, P. V. Afonine, G. Bunkóczi, V. B. Chen, I. W. Davis, N. Echols, J. J. Headd, L.-W. Hung, G. J. Kapral, R. W. Grosse-Kunstleve, A. J. McCoy, N. W. Moriarty, R. Oeffner, R. J. Read, D. C. Richardson, J. S. Richardson, T. C. Terwilliger and P. H. Zwart, *Acta Crystallogr D Biol Crystallogr*, 2010, 66, 213–221.

7 G. M. Sheldrick, *Acta Crystallogr A*, 2008, 64, 112–122.

8 P. Emsley and K. Cowtan, *Acta Crystallogr D Biol Crystallogr*, 2004, 60, 2126–2132.

9 A. Thorn, B. Dittrich and G. M. Sheldrick, *Acta Crystallogr A*, 2012, 68, 448–451.

10 V. B. Chen, W. B. Arendall, J. J. Headd, D. A. Keedy, R. M. Immormino, G. J. Kapral, L. W. Murray, J. S. Richardson and D. C. Richardson, *Acta Crystallogr D Biol Crystallogr*, 2010, 66, 12–21.

11 W. Kabsch and C. Sander, *Biopolymers*, 1983, 22, 2577–2637.

Table S1. Oligonucleotides used for site-directed mutagenesis of TM1459.

No.	Sequence (5'-3')	Length	Use
1	AGCCATCCGTGGGAACATGAAATTTTC	27	Forward primer for H52X, H54X
2	CGGATGGCTTGCGCGATCAATCAGACCACCCGGTT	27	Reverse primer for H52A
3	CGGTGCGCTATGGCGATCAATCAGACCACCCGGTT	35	Reverse primer for H54A
4	TGGGAAGCAGAAATTTTCGTGCTGAAAGGCAAAC	34	Forward primer for H58A
5	CGGATGGCTATGGCGATCAATCAGACCACCCGGTT	35	Reverse primer for H58X
6	GGCTTTCGCAACGATACCGATAGCGAAG	28	Forward primer for H92A
7	TGCGATTTCATTCGGTTCCACGAAGATG	28	Reverse primer for H92A
8	TGGGAACATGAAATTTTCGTGCTGAAAGGCAAAC	34	Forward primer for H52A
9	CGGTGCGCTTGCGCGATCAATCAGACCACCCGGTT	35	Reverse primer for H52A/H54A
10	TGGGAAGCAGAAATTTTCGTGCTGAAAGGCAAAC	34	Forward primer for H58A
11	CGGATGGCTTGCGCGATCAATCAGACCACCCGGTT	35	Reverse primer for H52A
12	CGGTGCGCTATGGCGATCAATCAGACCACCCGGTT	35	Reverse primer for H54A
13	GGCTTTCGCAACGATACCGATAGCGAAG	28	Forward primer for H92A
14	TGCGATTTCATTCGGTTCCACGAAGATG	35	Reverse primer for H92A
15	TTTCTGGATCTGATTCCGAAAGAAGGCGGAGAATGA	36	Forward primer for C106D
16	AATCAGATCCAGAAATTCCACTTCGCTATCGGTATCG	37	Reverse primer for C106D
17	TTTCTGGAACTGATTCCGAAAGAAGGCGGAGAATGA	36	Forward primer for C106E
18	AATCAGTTCCAGAAATTCCACTTCGCTATCGGTATCG	37	Reverse primer for C106E
19	TTTCTGCATCTGATTCCGAAAGAAGGCGGAGAATGA	36	Forward primer for C106H
20	AATCAGATGCAGAAATTCCACTTCGCTATCGGTATCG	37	Reverse primer for C106H
21	TTTCTGATGCTGATTCCGAAAGAAGGCGGAGAATGA	36	Forward primer for C106M
22	AATCAGCATCAGAAATTCCACTTCGCTATCGGTATCG	37	Reverse primer for C106M
23	TTTCTGCAGCTGATTCCGAAAGAAGGCGGAGAATGA	36	Forward primer for C106Q
24	AATCAGCTGCAGAAATTCCACTTCGCTATCGGTATCG	37	Reverse primer for C106Q
25	TGATGGCACTGTTTACGGTGGAACCGGGTGGTCTG	35	Forward primer for R39A
26	AACAGTGCCATCACAAAGTTCGGTGCATCTTTCAG	35	Reverse primer for R39A
27	TGATGAAACTGTTTACGGTGGAACCGGGTGGTCTG	35	Forward primer for R39K
28	AACAGTTTCATCACAAAGTTCGGTGCATCTTTCAG	35	Reverse primer for R39K
29	TGATGATGCTGTTTACGGTGGAACCGGGTGGTCTG	35	Forward primer for R39M
30	AACAGCATCATCACAAAGTTCGGTGCATCTTTCAG	35	Reverse primer for R39M
31	TGATGCAGCTGTTTACGGTGGAACCGGGTGGTCTG	35	Forward primer for R39Q
32	AACAGCTGCATCACAAAGTTCGGTGCATCTTTCAG	35	Reverse primer for R39Q

Table S2. Asymmetric hydrogenation of ketone with the 2-His dyad bearing mutants.[a]

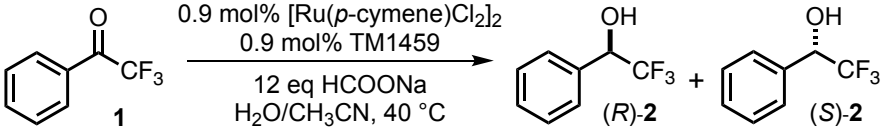

Entry	TM1459 Variant	Yield (%)[b]	*ee* (%)[b]
1	H52A/H54A	13	5(*R*)
2	H52A/H58A	17	8(*R*)
3	H54A/H58A	9	11(*R*)
4	H58A/H92A	20	15(*R*)

[a]Reaction conditions: TM1459 (0.15 mM), [Ru(*p*-cymene)Cl_2]$_2$ (0.15 mM), and substrate **1** (17 mM) in H_2O/CH_3CN (9:1) for 48h at 40 °C and pH 5. [b]The yield and enantiomeric excesses (*ee*) were determined by chiral HPLC analysis.

Table S3. Sodium formate concentration dependence of **58H** and **58H**/C106E mutants in asymmetric hydrogenation.[a]

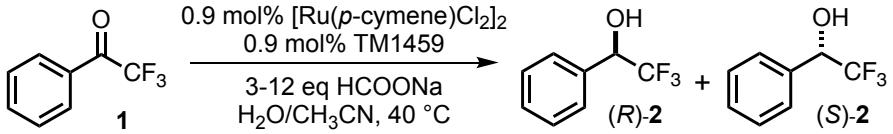

Entry	TM1459 Variant	Formate (equiv.)	Yield (%)[b]	*ee* (%)[b]
1		12	31	61 (*S*)
2	**58H**	6	16	61 (*S*)
3		3	14	68 (*S*)
4		12	80	81 (*S*)
5	**58H**/C106E	6	63	87 (*S*)
6		3	56	91 (*S*)

[a]Reaction conditions: TM1459 (0.15 mM), [Ru(*p*-cymene)Cl_2]$_2$ (0.15 mM), and substrate **1** (17 mM) in H_2O/CH_3CN (9:1) for 48h at 40 °C and pH 5. [b]The yield and enantiomeric excesses (*ee*) were determined by chiral HPLC analysis.

Table S4. Data collection and refinement statistics.[a]

	58H/C106E [H52A/H54A/H92A/C106E (PDB code: 9XS8)]	R39K/**58H**/C106E [R39K/H52A/H54A/H92A/C106E (PDB code: 9XS9)]	R39M/**58H**/C106E [R39M/H52A/H54A/H92A/C106E (PDB code: 9XSA)]
Dataset			
X-ray source	Spring-8 BL44XU	Spring-8 BL44XU	Spring-8 BL44XU
Space group	$P2_12_12_1$	$P2_12_12_1$	$P2_12_12_1$
Unit cell	a = 50.814 Å, b = 57.632 Å, c = 74.501 Å, $\alpha = \beta = \gamma$ = 90°	a = 50.148 Å, b = 58.096 Å, c = 74.539 Å, $\alpha = \beta = \gamma$ = 90°	a = 50.197Å, b = 57.755 Å, c = 75.023 Å, $\alpha = \beta = \gamma$ = 90°
Wavelength	0.899995 Å	0.899995 Å	0.899995 Å
Resolution	37.25 to 1.265 Å	45.83 to 1.087 Å	45.77 to 1.423 Å
No. reflection (total/unique)	384608/112232	587689/174458	269165/78202
Redundancy[b]	3.43 (3.22)	3.37 (3.05)	3.44 (3.48)
Completeness[b]	99.4% (98.9%)	98.6% (95.4%)	99.0% (97.8%)
R_{merge}[b]	4.4% (58.1%)	5.8% (18.3%)	6.2%/61.6%
I/σ[b]	13.79 (2.03)	12.8 (4.89)	10.15 (2.08)
CC(1/2)	99.8% (72.3%)	99.4% (96.2%)	99.7% (73.2%)
Refinement			
R_{work}/R_{free}	0.1474/0.1981	0.1317/0.1605	0.1884/0.2505
No. of protein/solvent atoms[c]	1814/201	1828/294	1764/118
No. of metal ion atoms	2	2	2
B-factors of protein/solvent	23.8/43.0	16.2/34.4	26.5/38.3
B-factors of metal ions	48.1	19.5	50.9
r.m.s.d. bond/angle	0.0098/1.91	0.0127/1.82	0.0069/1.42
Ramchandran favored/allowed[d]	98.2%/1.8%	99.1%/0.9%	98.7%/1.3%

[a]A single crystal was used for all of structures. [b]Values in parentheses are for highest-resolution shell. [c]Hydrogen atoms not included. [d]Values are calculated by Molprobity.

Table S5. Missing residues and atoms.

58H/C106E [H52A/H54A/H92A/C106E (PDB code: 9XS8)]
Missing residues
Chain B, Gly(-3)–Gly(0), Glu114
Missing atoms
Chain A, Gln12 (Cγ, Cδ, Oε1, Nε2), Lys66 (Cγ, Cδ, Cε, Nζ), Gln73 (Cγ, Cδ, Oε1, Nε2)
Chain B, Asp17 (Cγ, Oδ1, Oδ2), Lys18 (Cγ, Cδ, Cε, Nζ), Lys31 (Cδ, Cε, Nζ)
R39K/**58H**/C106E [R39K/H52A/H54A/H92A/C106E (PDB code: 9XS9)]
Missing residues
Chain B, Gly(-3)–Gly(0)
Missing atoms
Chain A, Gln12 (Cγ, Cδ, Oε1, Nε2)
Chain B, Asp17 (Cγ, Oδ1, Oδ2), Lys18 (Cγ, Cδ, Cε, Nζ) Glu44(Cγ, Cδ, Oε1, Oε2)
R39M/**58H**/C106E [R39M/H52A/H54A/H92A/C106E (PDB code: 9XSA)]
Missing residues
Chain B, Gly(-3)–Gly(0), Glu114
Missing atoms
Chain A, Gln12 (Cγ, Cδ, Oε1, Nε2), Lys18 (Cγ, Cδ, Cε, Nζ), Arg20 (Cγ, Cδ, Nε, Cζ, Nη1, Nη2), Asp50 (Cγ, Oδ1, Oδ2), Lys66 (Cγ, Cδ, Cε, Nζ), Gln73 (Cγ, Cδ, Oε1, Nε2), Thr77 (Oγ1, Cγ2), Glu80 (Cγ, Cδ, Oε1, Oε2), Glu90 (Cγ, Cδ, Oε1, Oε2)
Chain B, Asp17 (Cγ, Oδ1, Oδ2), Lys18 (Cγ, Cδ, Cε, Nζ), Arg23 (Cγ, Cδ, Nε, Cζ, Nη1, Nη2), Lys31 (Cγ, Cδ, Cε, Nζ), Ser53 (Oγ1), Glu79 (Cγ,Cδ, Oε1, Oε2), Lys110 (Cγ, Cδ, Cε, Nζ), Glu111 (Cγ, Cδ, Oε1, Oε2)

Table S6. Interatomic distances and bond angles in the crystal structures (Ru ion and coordinating atoms).

58H/C106E [H52A/H54A/H92A/C106E (PDB code: 9XS8)]				
Chain A				
Bond Lengths[a]				
	His58(Nε)	Glu106(Oε1)	Glu106(Oε2)	O1
Ru	2.14 (0.04)	3.48 (0.04)	3.13 (0.05)	2.81 (0.04)
Angles[a]				
Ru	His58(Nε)	Glu106(Oε1)	Glu106(Oε2)	O1
His58(Nε)				
Glu106(Oε1)	89.7 (1.4)			
Glu106(Oε2)	85.5 (1.4)	37.9 (1.0)		
O1	77.9 (1.3)	109.9 (1.3)	72.1 (1.3)	
Chain B				
Bond Lengths[a]				
	His58(Nε)	Glu106(Oε1)	Glu106(Oε2)	O1
Ru	2.21 (0.04)	3.15 (0.06)	4.16 (0.10)	2.60 (0.07)
Angles[a]				
Ru	His58(Nε)	Glu106(Oε1)	Glu106(Oε2)	O1
His58(Nε)				
Glu106(Oε1)	86.3 (1.7)			
Glu106(Oε2)	92.9 (1.5)	32.0 (1.8)		
O1	79.0 (1.6)	107.6 (2.0)	78.3 (1.5)	

[a]Distances and angles are given in Å and degrees (°), estimated errors are given in parentheses.

R39K/**58H**/C106E [R39K/H52A/H54A/H92A/C106E (PDB code: 9XS9)]

Chain A

Bond Lengths[a]

	His58(Nε)	Glu106A(Oε1)	Glu106A(Oε2)	Glu106B(Oε1)	Glu106B(Oε2)	O1
Ru	2.10 (0.02)	3.07 (0.02)	2.11 (0.02)	2.47 (0.05)	3.51 (0.08)	2.80 (0.02)

Angles[a]

Ru	His58(Nε)	Glu106A(Oε1)	Glu106A(Oε2)	Glu106B(Oε1)	Glu106B(Oε2)	O1
His58(Nε)						
Glu106A(Oε1)	88.2 (0.5)					
Glu106A(Oε2)	83.6 (0.7)	46.2 (0.6)				
Glu106B(Oε1)	87.7 (0.9)					
Glu106B(Oε2)	94.2 (1.2)			38.1 (1.7)		
O1	76.7 (0.5)	126.7 (0.5)	81.1 (0.7)	101.9 (1.4)	67.1 (1.2)	

Chain B

Bond Lengths[a]

	His58(Nε)	Glu106A(Oε1)	Glu106A(Oε2)	Glu106B(Oε1)	Glu106B(Oε2)	O1
Ru	2.10 (0.01)	3.32 (0.02)	2.34 (0.03)	4.22 (0.06)	2.51 (0.08)	2.51 (0.08)

Angles[a]

Ru	His58(Nε)	Glu106A(Oε1)	Glu106A(Oε2)	Glu106B(Oε1)	Glu106B(Oε2)	O1
His58(Nε)						
Glu106A(Oε1)	87.4 (0.6)					
Glu106A(Oε2)	82.9 (0.7)	41.7 (0.5)				
Glu106B(Oε1)	93.9 (0.9)					
Glu106B(Oε2)	88.4 (1.1)			24.3 (1.9)		
O1	79.5 (0.5)	124.7 (0.4)	83.3 (0.6)	77.9 (0.7)	100.1 (1.6)	

[a]Distances and angles are given in Å and degrees (°), estimated errors are given in parentheses.

R39M/**58H**/C106E [R39M/H52A/H54A/H92A/C106E (PDB code: 9XS8)]				
Chain A				
Bond Lengths[a]				
	His58(Nε)	Glu106(Oε1)	Glu106(Oε2)	O1
Ru	2.20 (0.06)	3.18 (0.07)	2.53 (0.04)	2.76 (0.1)
Angles[a]				
Ru	His58(Nε)	Glu106(Oε1)	Glu106(Oε2)	O1
His58(Nε)				
Glu106(Oε1)	94.8 (2.2)			
Glu106(Oε2)	80.3 (2.3)	43.3 (2.1)		
O1	70.7 (2.3)	118.4 (2.3)	75.1 (2.4)	
Chain B				
Bond Lengths[a]				
	His58(Nε)	Glu106(Oε1)	Glu106(Oε2)	O1
Ru	2.16 (0.07)	3.49 (0.07)	3.09 (0.08)	2.41 (0.08)
Angles[a]				
Ru	His58(Nε)	Glu106(Oε1)	Glu106(Oε2)	O1
His58(Nε)				
Glu106(Oε1)	90.3 (2.6)			
Glu106(Oε2)	87.3 (2.3)	38.5 (1.6)		
O1	71.9 (2.6)	126.0 (2.9)	88.9 (3.1)	

[a]Distances and angles are given in Å and degrees (°), estimated errors are given in parentheses.

Table S7. pH dependence with the R39K/**58H**/C106E mutant in the asymmetric hydrogenation.[a]

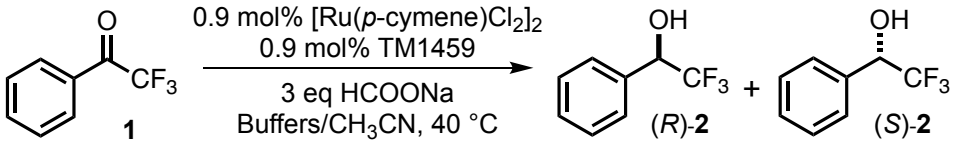

Entry	TM1459 Variant	pH	Yield (%)[b]	*ee* (%)[b]
1	R39K/**58H**/C106E	4.0[c]	14	9 (*S*)
2		5.0[d]	60	94 (*S*)
3		6.0[d]	71	95 (*S*)
4		7.0[d]	71	94 (*S*)
5		8.0[e]	15	53 (*S*)
6		9.0[e]	4	50 (*S*)

[a]Reaction conditions: TM1459 (0.15 mM), [Ru(*p*-cymene)Cl_2]$_2$ (0.15 mM), and substrate **1** (17 mM) in Buffers/CH_3CN (9:1) for 48h at 40 °C. [b]The yield and enantiomeric excesses (*ee*) were determined by chiral HPLC analysis. [c]50mM acetate, [d]50mM phosphate, [e]50mM borate.

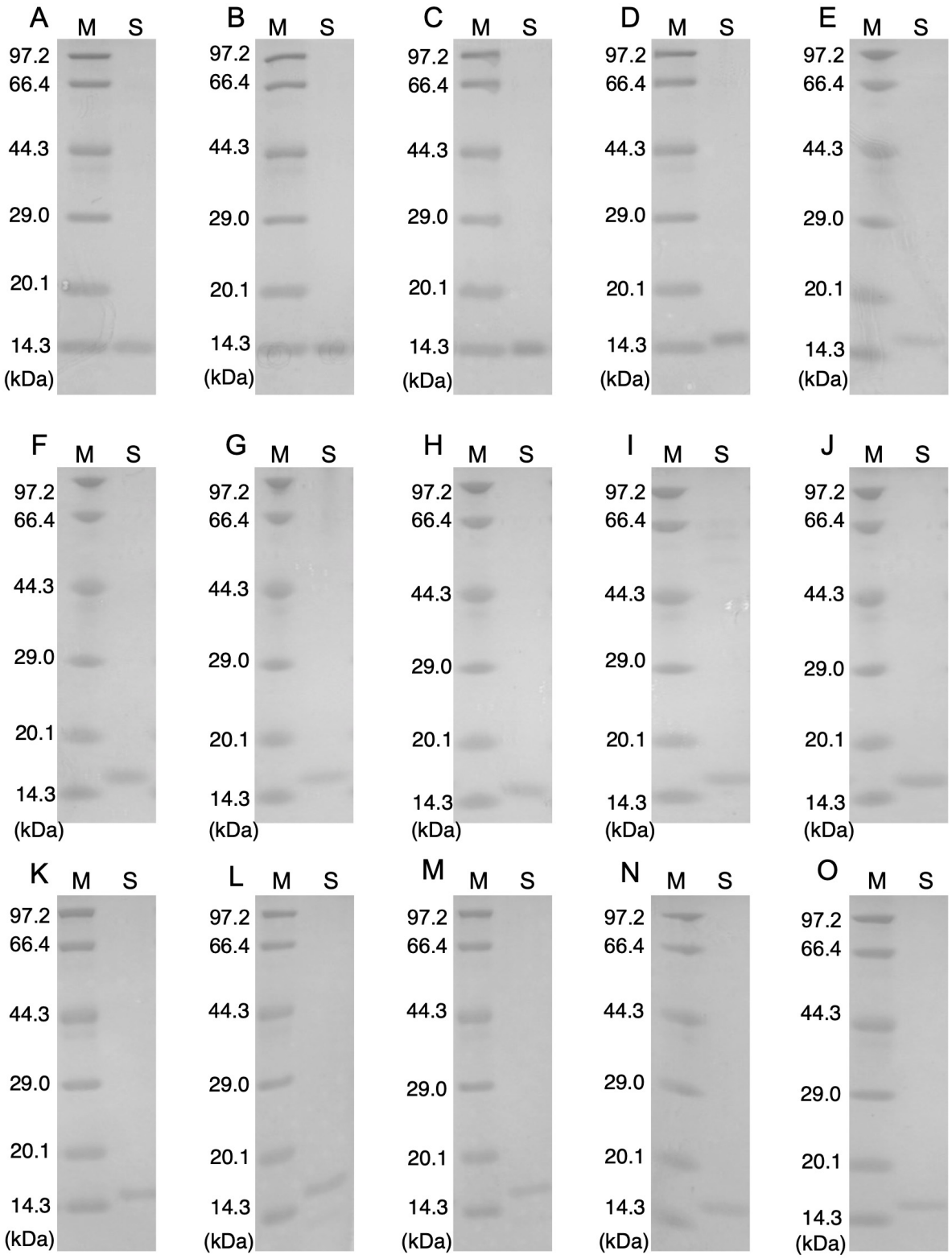

Fig. S1 SDS-PAGE (Bis-tris 10 % acrylamide gel) analysis of the apo-TM1459 isoforms used in this study. (A) H52A/H54A; (B) H52A/H58A; (C) H54A/H58A; (D) H58A/H92A; (E) H54A/H58A/H92A; (F) H52A/H58A/H92A; (G) H52A/H54A/H92A; (H) H52A/H54A/H58A; (I) H52A/H54A/H92A/C106D; (J) H52A/H54A/H92A/C106E; (K) H52A/H54A/H92A/C106H; (L) H52A/H54A/H92A/C106M; (M) H52A/H54A/H92A/C106Q; (N) R39K/H52A/H54A/H92A/C106E; (O) R39M/H52A/H54A/H92A/C106E.

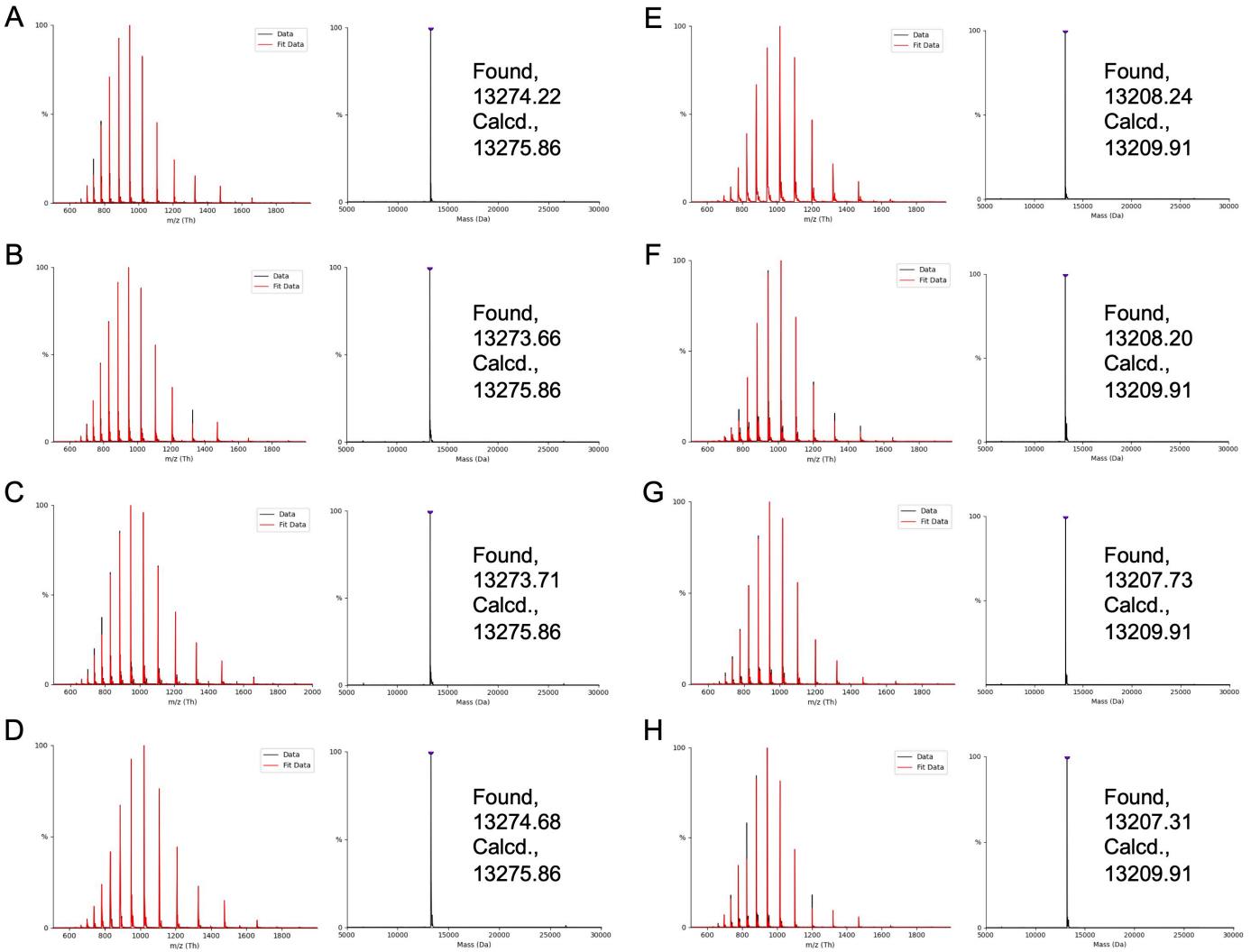
A
Data
Fit Data
m/z (Th)
Mass (Da)
Found,
13274.22
Calcd.,
13275.86
B
Found,
13273.66
Calcd.,
13275.86
C
Found,
13273.71
Calcd.,
13275.86
D
Found,
13274.68
Calcd.,
13275.86
E
Found,
13208.24
Calcd.,
13209.91
F
Found,
13208.20
Calcd.,
13209.91
G
Found,
13207.73
Calcd.,
13209.91
H
Found,
13207.31
Calcd.,
13209.91

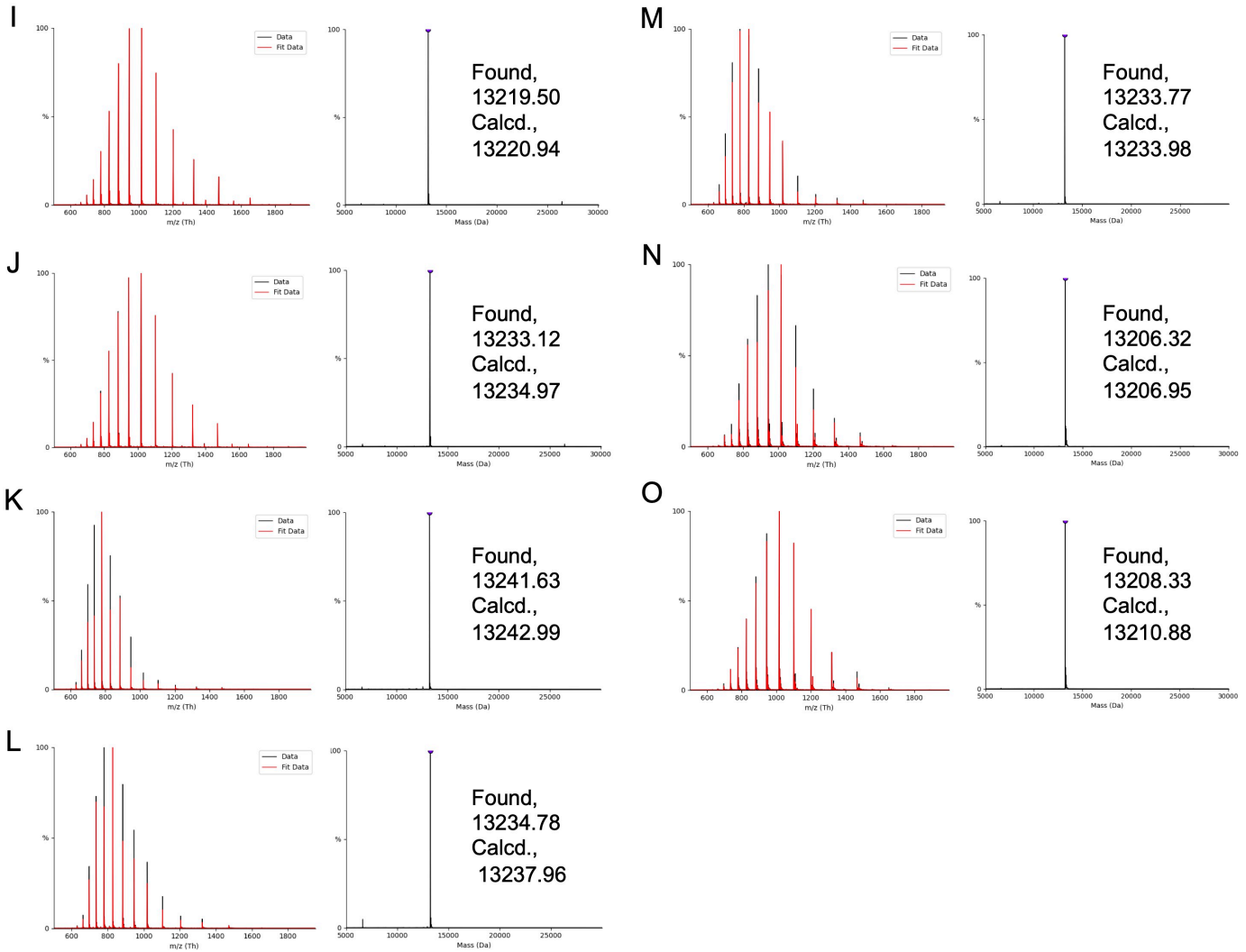

Fig. S2 Non-deconvoluted (left) and deconvoluted (right) ESI-MS spectra of multiply-charged ions of the apo-TM1459 isoforms used in this study. (A) H52A/H54A; (B) H52A/H58A; (C) H54A/H58A; (D) H58A/H92A; (E) H54A/H58A/H92A; (F) H52A/H58A/H92A; (G) H52A/H54A/H92A; (H) H52A/H54A/H58A; (I) H52A/H54A/H92A/C106D; (J) H52A/H54A/H92A/C106E; (K) H52A/H54A/H92A/C106H; (L) H52A/H54A/H92A/C106M; (M) H52A/H54A/H92A/C106Q; (N) R39K/H52A/H54A/H92A/C106E; (O) R39M/H52A/H54A/H92A/C106E.

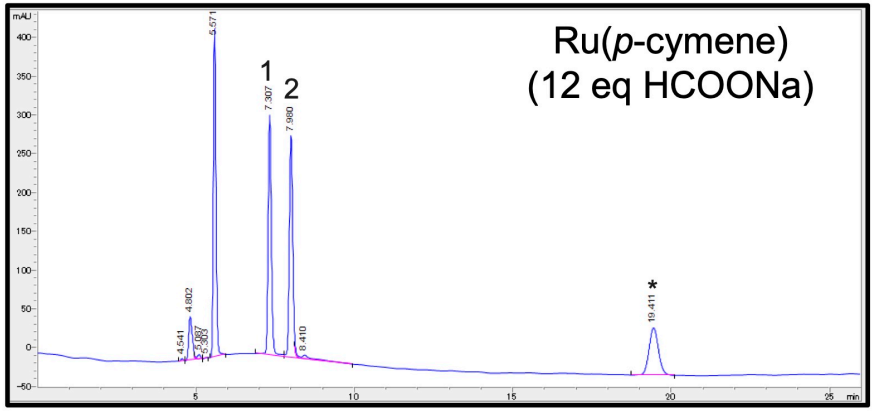

	Time (min)	Area (mAU)	Height	Width	Symmetry	Area (%)
1	7.307	2143	309.3	0.1068	0.848	50.401
2	7.98	2108.9	284.9	0.1144	0.876	49.599

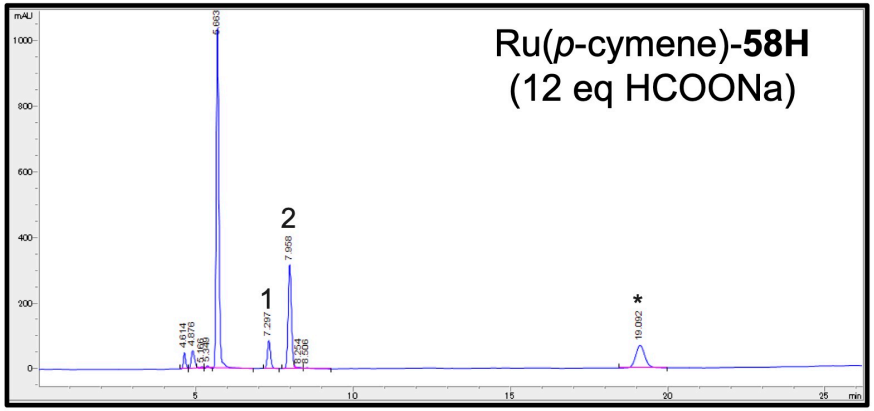

	Time (min)	Area (mAU)	Height	Width	Symmetry	Area (%)
1	7.297	573.3	85.4	0.1044	0.852	19.941
2	7.958	2301.8	314.7	0.1153	0.87	80.059

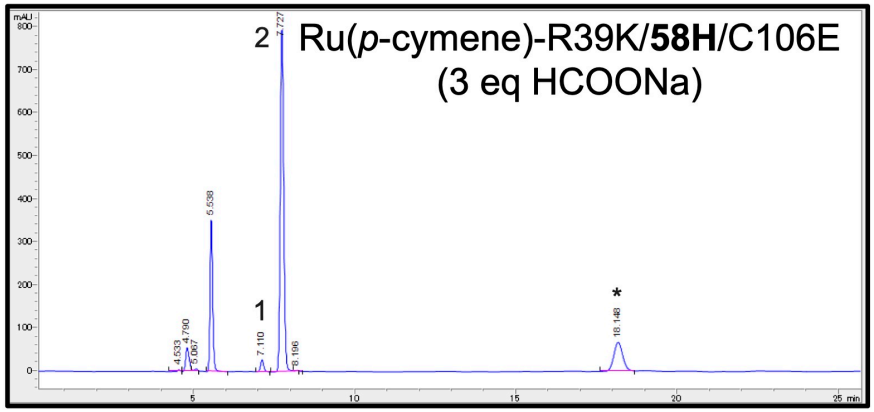

	Time (min)	Area (mAU)	Height	Width	Symmetry	Area (%)
1	7.11	186.4	27.7	0.1044	0.847	3.102
2	7.727	5823.1	797.6	0.1132	0.872	96.898

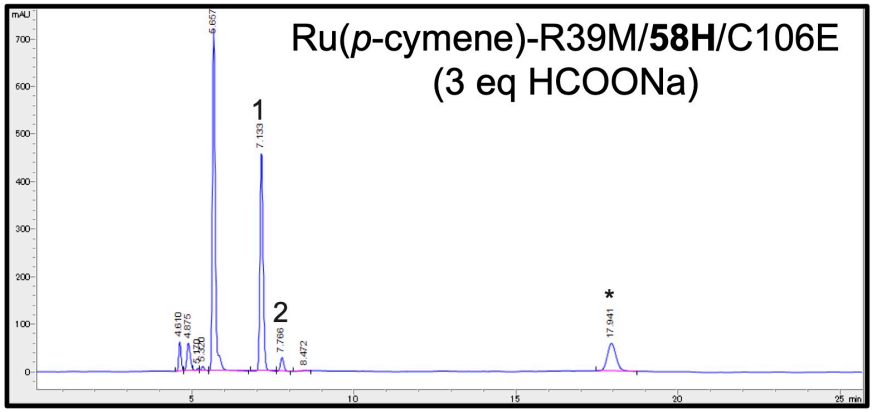

	Time (min)	Area (mAU)	Height	Width	Symmetry	Area (%)
1	7.133	3101.5	459.3	0.1048	0.846	93.768
2	7.766	206.1	29.1	0.1105	0.866	6.232

Fig. S3 Separation of product stereoisomers for the asymmetric hydrogenation reaction of trifluoro acetophenone and formic acid catalyzed by selected mutant on chiral normal-phase chromatography. Separation of product, 1, (*R*)-(–)-isomer; 2, (*S*)-(+)-isomer; *, internal standard.

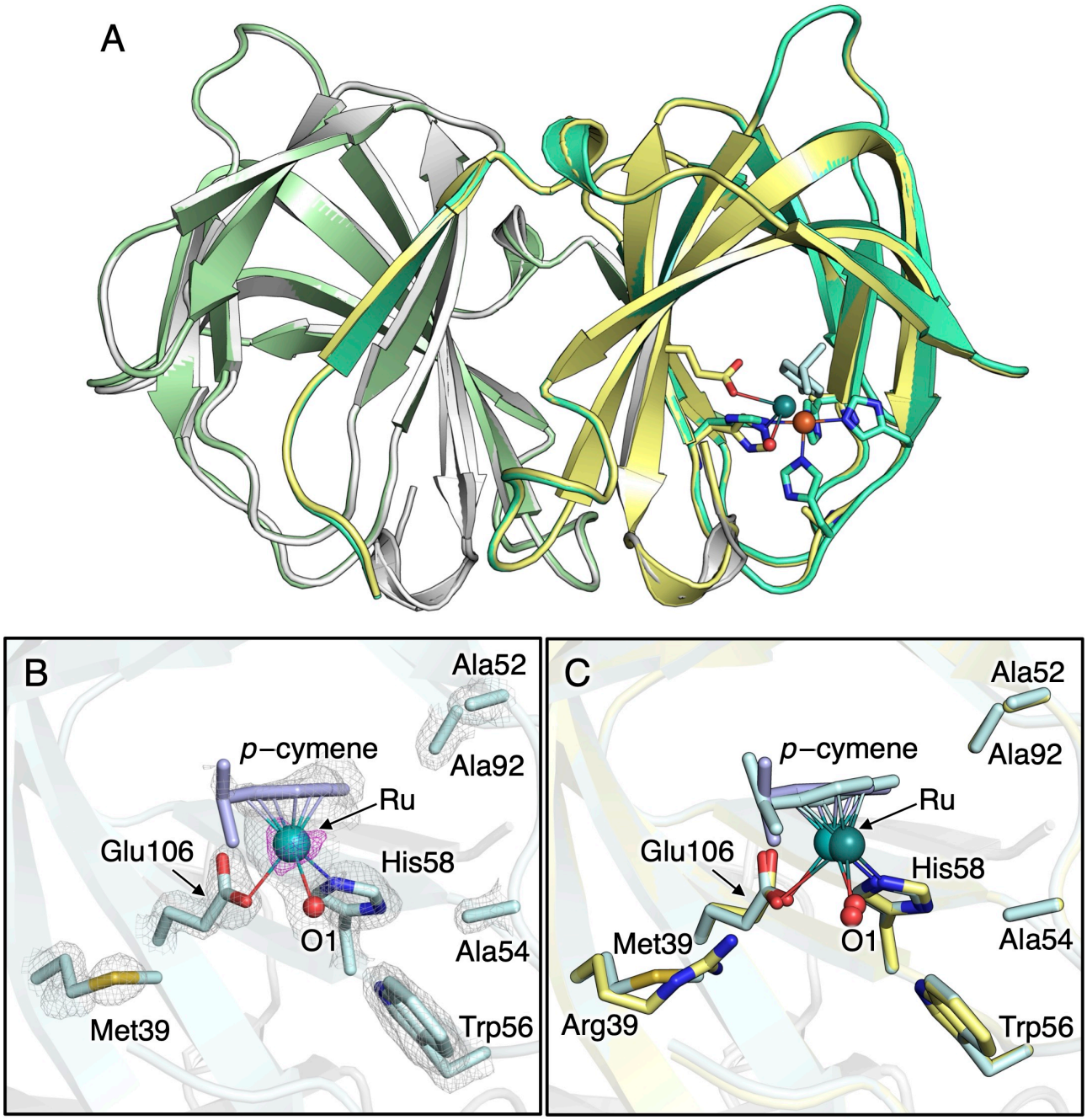

Fig. S4 (A) Overall structure of Ru(*p*-cymene)-bound **58H**/C106E (yellow and white, PDB code: 9XS8) superimposed with that of wild type (green, PDB code: 9JEU). (B) The active site structure of Ru(*p*-cymene)-bound R39M/**58H**/C106E (chain A). (C) Structure of the active site of Ru(*p*-cymene)-bound R39M/**58H**/C106E (blue) superimposed with that of Ru(*p*-cymene)-bound **58H**/C106E (yellow). The protein main chain is displayed as a ribbon, Ru ions are shown as green spheres, and the selected amino acids is indicated as stick. The 2FoFc and anomalous maps contoured at 1.5σ and 5.0σ are shown in gray and magenta, respectively.